


## Critical behavior of magnetic polymers in two and three dimensions

Damien Paul Foster<sup>✉\*</sup>

*Centre for Computational Science and Mathematical Modelling, Coventry University, Coventry CV1 5FB, United Kingdom*

Debjyoti Majumdar<sup>✉†</sup>

*Institute of Physics, Bhubaneswar, Odisha 751005, India  
and Homi Bhabha National Institute, Training School Complex, Anushakti Nagar, Mumbai 400094, India*

 (Received 27 May 2021; revised 12 July 2021; accepted 28 July 2021; published 16 August 2021)

We explore the critical behavior of two- and three-dimensional lattice models of polymers in dilute solution where the monomers carry a magnetic moment which interacts ferromagnetically with near-neighbor monomers. Specifically, the model explored consists of a self-avoiding walk on a square or cubic lattice with Ising spins on the visited sites. In three dimensions we confirm and extend previous numerical work, showing clearly the first-order character of both the magnetic transition and the polymer collapse, which happen together. We present results in two dimensions, where the transition is seen to be continuous. Finite-size scaling is used to extract estimates for the critical exponents and the transition temperature in the absence of an external magnetic field.

DOI: [10.1103/PhysRevE.104.024122](https://doi.org/10.1103/PhysRevE.104.024122)

### I. INTRODUCTION

Self-avoiding walk models on lattices have been used for several decades as good models for polymers in solution [1]. Short-ranged interactions between nearest-neighbor visited lattice sites are introduced to mimic the effects of solvent quality, and other interactions may be introduced to account for other effects. Canonically, if the interactions are short-ranged and the walks are studied in their infinite length limit, there should exist a universality where the critical behavior is insensitive to details of the model [2–4]. An early indication that things are not so simple arose in the study of the two-dimensional  $O(n \rightarrow 0)$  model introduced by Blote and Nienhuis [5], more recently known under the title of vertex interacting self-avoiding walk [6–9]. They found that in this model, despite having short-ranged interactions, corresponding to noncrossing doubly visited sites, the critical exponents were not the same as those found previously for the interacting self-avoiding walk (ISAW). This lack of universality is due to a fractal dimension for the walk which equals that of the lattice, giving rise to a critical point with a first-order character [6,10].

In the models described above, the walks are neutral and nonmagnetic. In this paper we look at the critical behavior of polymers where each monomer has a magnetic moment (spin) which may be either “up” or “down.” The walk is modeled by a self-avoiding walk on a square [two-dimensional (2D)] or cubic [three-dimensional (3D)] lattice, and the spins sit on the occupied lattice sites and interact via the standard ferromagnetic Ising Hamiltonian (Fig. 1). The spins interact with all spins that are on adjacent sites (including along the walk). The

only energy taken into account is this Ising interaction energy; however, the entropy will be the sum of the spin entropy and the walk configurational entropy. This model was introduced by Garel *et al.* [11] and studied in three dimensions.

Magnetic polymers have been used as models to understand epigenomic microphase separation in proteins in the cell nucleus [12–14], although the model used a three-state Potts model, rather than an Ising model as used here. The equilibrium model was able to reproduce some of the results seen in the *in vivo* experiments, but it was shown that it was necessary to consider nonequilibrium effects to understand the behavior in the cell.

Possible experimental realizations of polymers with magnetic monomer-monomer interactions include magnetic filaments where magnetic nanoparticles (ferromagnetic or paramagnetic) are cross-linked by polymers to form linear structures [15]. The magnetic particles can be considered equivalent to the monomers in a polymer and the cross-linking polymers as the bonds which bind them together. One experimental realization involves “biotemplating,” which involves bioengineering flagellar filaments from *Salmonella* bacteria to contain magnetic nanoparticles [16]. Inspired by biological flagella and cilia, artificial cilia have been constructed using thermoresponsive phase transitions of magnetic nanoparticles decorated with polymers leading to an ordered assembly [17].

The partition function for a walk of length  $N$  is

$$Z_N = \sum_{\Omega_N} \sum_{\{\sigma_i = \pm 1\}} \exp \left( \beta J \sum_{\langle i, j \rangle} \sigma_i \sigma_j + \beta h \sum_i \sigma_i \right), \quad (1)$$

where  $\Omega_N$  is the set of self-avoiding walks of length  $N$ ,  $\sigma_i = \pm 1$  are the two-state Ising spins, as usual  $\langle i, j \rangle$  indicates that the sum is over pairs of spins which are nearest neighbors on the lattice,  $J$  is the spin-spin interaction energy,  $h$  is a magnetic

\*ab5651@coventry.ac.uk

†debjyoti@iopb.res.in

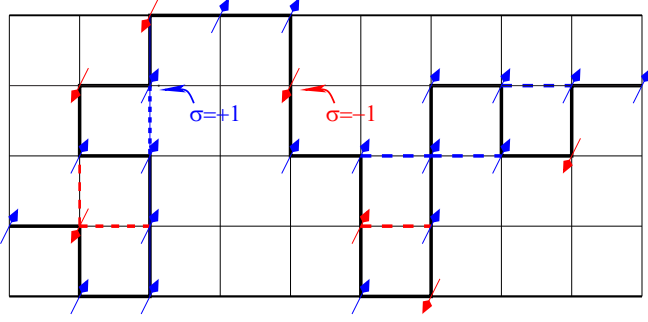


FIG. 1. Magnetic walk model in two dimensions.

field, and  $\beta = 1/kT$  as usual (with  $k$  being the Boltzmann constant). In what follows we set  $J/k = 1$ .

It is important to be clear that the equilibrium is defined by a minimization of the free energy:

$$F = E_{\text{Ising}} - T(S_{\text{Ising}} + S_{\text{SAW}}), \quad (2)$$

In other words, the polymer configurations and the spin states are both fluctuating quantities in thermal equilibrium. There have been many studies where either one or the other are frozen, i.e., the spin configuration is quenched and the walk configurations are studied [18] or the self-avoiding walk configuration is quenched and the behavior of the Ising model on the resulting fractal is studied [19–21], but the current situation has been much less studied. The model described here was introduced by Garel *et al.* [11] and studied by both mean-field theory (MFT) and multiple Markov chain Monte Carlo methods [22,23] in three dimensions. The MFT suggested that at low magnetic fields there is a simultaneous first-order magnetic and collapse transition. In the limit of infinite magnetic field, the model is simply the usual ISAW model, where the transition is tricritical [2], and this extends into a line of tricritical transitions as  $h$  is lowered. The first-order and tricritical lines are separated by a multicritical point. Their numerical results tend to support the MFT picture. The main evidence for the behavior at  $h = 0$  was a rapid variation of the magnetization and radius of gyration as the transition was approached and linear scaling of the specific heat as an indicator of the first-order transition.

Another related model was studied by Luo and coworkers [24–29] in zero external magnetic field in three dimensions on the cubic lattice. In this case they allowed the bonds to fluctuate in length, but pairs of spins only interacted if they were nearest neighbors, either along the chain or not. Luo concluded that the transition was critical and gave an estimate of the critical temperature and some exponents [28].

In this paper we revisit the three-dimensional model and investigate the two-dimensional model using a variant of the pruned-enriched Rosenbluth method (PERM) [30] known as flatPERM [31] to stochastically enumerate the number of configurations as a function of the number of magnetic energy indexed by  $n_i$  below and the magnetization indexed by  $n_s$  from which we can construct the partition function, given by

$$Z_N = \sum_{n_i=-n_{i,\min}}^{n_{i,\max}} \sum_{n_s=-N-1}^{N+1} c_{N,n_i,n_s} \exp\left(\frac{1}{T}(n_i + hn_s)\right), \quad (3)$$

where  $n_i = \sum_{(i,j)} \sigma_i \sigma_j$  is the difference between the number of satisfied nearest-neighbor bonds and the number of unsatisfied bonds, and  $n_s = \sum_{i=0}^N \sigma_i$  is the difference between the number of up spins and the number of down spins. The coefficient  $c_{N,n_i,n_s}$  is the number of walks of length  $N$  with  $n_i$  and  $n_s$  being fixed.

The internal energy  $\langle E \rangle$  and the square magnetization  $\langle M^2 \rangle$  can be directly calculated (the magnetization is expected to be zero on average at all temperatures by symmetry). As we are also interested in the fourth-order Binder cumulant [32], we also need to calculate  $\langle M^4 \rangle$ . These averages can be calculated in the usual way using the expressions

$$\langle E^x \rangle = \frac{1}{Z_N} \sum_{n_i,n_s} n_i^x c_{N,n_i,n_s} \exp\left(\frac{1}{T}(n_i + hn_s)\right), \quad (4)$$

$$\langle M^x \rangle = \frac{1}{Z_N} \sum_{n_i,n_s} n_s^x c_{N,n_i,n_s} \exp\left(\frac{1}{T}(n_i + hn_s)\right). \quad (5)$$

The fourth-order Binder cumulant is defined as [33,34]

$$U_m = 1 - \frac{\langle M^4 \rangle}{3\langle M^2 \rangle^2}. \quad (6)$$

As the number of spins tends to infinity,  $U_m \rightarrow 0$  from above for  $T > T_c$  and  $U_m \rightarrow 2/3$  from below for  $T < T_c$ , at  $T_c$ ,  $U_m \rightarrow U^*$ , which is a unique number related to geometry and boundary conditions and so is not universal [35,36]. Crossings of the Binder cumulant are indicative of a phase transition [33].

A phase transition is also indicated, typically, by a divergence of the specific heat defined through

$$C = \frac{1}{N} \frac{\partial E}{\partial T} = \frac{\partial^2 f}{\partial T^2}, \quad (7)$$

where  $f$  is the free energy per spin. This leads to the alternative expression for the specific heat,  $C = \frac{1}{NT^2} (\langle E^2 \rangle - \langle E \rangle^2)$ . Finite-size estimates of the transition temperature can be obtained from the peaks of  $C$ .

Any other quantity can be calculated if the table of values is accumulated as the configurations are enumerated. Here we have calculated the radius of gyration squared:

$$R_g^2 = \frac{1}{Z_N} \sum_{n_i,n_s} r_{N,n_i,n_s} \exp\left(\frac{1}{T}(n_i + hn_s)\right), \quad (8)$$

where

$$r_{N,n_i,n_s} = \sum_{i \in \Omega_{N,n_i,n_s}} \langle \vec{r}_i - \langle \vec{r}_i \rangle \rangle^2 \quad (9)$$

and  $i$  labels the chain in the set  $\Omega_{N,n_i,n_s}$  of walks of length  $N$  with  $n_i$  and  $n_s$  being fixed. The average is done over the positions of the  $N + 1$  occupied sites of chain  $i$ .

In order to look at longer chain lengths, we can define partial partition functions for fixed  $n_i$ , but incorporating the magnetic field:

$$c_{N,n_i}^{\text{eff}} = \sum_{n_s=-N+1}^{N+1} c_{N,n_i,n_s} \exp\left(-\frac{h}{T}n_s\right). \quad (10)$$

Everything proceeds as before, but  $M^2$ ,  $M^4$ , and  $|M|$  need to be accumulated in the same way as  $R_g^2$  to enable weighted averages to be calculated later.

## II. SCALING RELATIONS

In polymer physics, the exponents have slightly different interpretations and sometimes expressions than for the Ising model, and in this model there is a risk of confusion between the two. In this section we take the opportunity to recall the relevant finite-scaling relations which will be used to identify the transition points and the critical exponent estimates, since we are working in the fixed length ensemble, and not the usual fixed lattice size ensemble.

If we cast the problem on an infinite lattice and control the length of the walk through a fugacity  $K$ , the partition function will be given by

$$\mathcal{Z} = \sum_{N=0}^{\infty} K^N Z_N. \quad (11)$$

The (average) length of the walk is governed by  $K$ , and  $\langle N \rangle \sim (K_c - K)^{-1}$  for  $K \leq K_c$ . The free energy per lattice site for  $K \leq K_c$  is 0, which is a reflection of the fractal nature of the walk. As a result one uses the free energy per monomer instead, and the correct scaling expression for the singular part of the free energy per monomer (and hence spin) is

$$f_s = b^{-d_H} \tilde{f}(kb^{y_1}, tb^{y_2}, hb^{y_h}), \quad (12)$$

where  $b$  is the linear scaling factor, and where the Hausdorff dimension of the walk is  $d_H \leq d$ . The  $\{y_i\}$  are the scaling dimensions [37]. We have defined the reduced dimensionless variables  $k = (K_c - K)/K_c$  and  $t = (T_c - T)/T_c$ . Typically, we identify  $d_H = y_1 = 1/\nu$ , where  $\nu$  is the geometric exponent given by

$$R \sim N^\nu. \quad (13)$$

$R$  is any typical linear dimension of the walk, e.g., radius of gyration, end-to-end distance, or hydrodynamic radius.

Taking two derivatives with respect to  $t$  and then setting  $tb^{y_2}$  constant gives

$$C \sim t^{y_1/y_2-2} \sim t^{-\alpha}, \quad (14)$$

where we have used  $d_H = y_1$ . Defining the crossover exponent  $\phi = y_2/y_1$  leads to the relation  $\alpha = 2 - 1/\phi$ , relevant for polymer models [38]. The exponent  $\phi$  is the crossover exponent.

In order to introduce the finite-size scaling relations we need, we identify the relevant scale factor as the radius of gyration  $r = \sqrt{\langle R_g^2 \rangle}$ , or alternatively  $N^\nu = N^{1/y_1}$ . Fixing  $N$  corresponds to fixing  $k$ , and using Eq. (12), we find the tricritical scaling expression:

$$f_s = N^{-1} \tilde{f}(kN, tN^\phi, hN^\Delta) = N^{-1} \Phi(tN^\phi, hN^\Delta), \quad (15)$$

where  $\Delta = y_h/y_1$ .

Fixing  $tN^\phi = x_{\max}$ , the value giving the maximum of  $C$ , and differentiating twice  $f_s$  again with respect to  $t$ , gives

$$C_{\max} \sim N^{-1+2\phi} \sim N^{\alpha\phi} \sim N^{\frac{\alpha}{2-\alpha}} \text{ and} \quad (16)$$

$$t \sim N^{-\phi}, \quad (17)$$

for sufficiently large  $N$ .

For a first-order transition, we expect  $C_{\max}$  to scale with the volume, which here is  $N$ , leading to  $\alpha = 1$  at the first-order transition expected in three dimensions and  $h = 0$ . This

is what was observed by Garel *et al.* [11] and is confirmed here. At the standard collapse transition (relevant for larger  $h$ ),  $\alpha = 0$  with logarithmic corrections [4,39].

We also use the scaling behaviors of  $m = \frac{1}{N+1} \sqrt{\langle M^2 \rangle}$  and  $r = \sqrt{\langle R_g^2 \rangle}$ .

For the magnetization, we expect either

$$m \sim (T_c - T)^\beta, \quad (18)$$

if the transition is critical, or a jump in  $m$ , if it is first order. The usual finite-size scaling for the ferromagnetic transition would be

$$\frac{1}{(N+1)^2} \langle M^2 \rangle = L^{-2\beta/\nu_2} \tilde{M}(tL^{\nu_2}). \quad (19)$$

The relevant length scale is again  $L = r = aN^\nu$ , and so

$$m = N^{-\beta\phi} \tilde{m}(tN^\phi). \quad (20)$$

Assuming the scaling behavior for  $r$  and  $m$  from Eqs. (13) and (20), we can define the scaling functions

$$\varphi_{R_g} = \frac{\log(r_N/r_{N'})}{\log(N/N')}, \quad \varphi_m = \frac{\log(m_N/m_{N'})}{\log(N/N')}. \quad (21)$$

Crossings of these functions give estimates of the  $T_c$  [40], which are expected to converge to the correct value as  $N \rightarrow \infty$ . Also, as  $N \rightarrow \infty$ , the values of these functions give  $\varphi_{R_g} \rightarrow \nu$  and  $\varphi_m \rightarrow -\beta\phi$ .

Another useful tool to use for estimating critical temperatures and, in the case of polymers, the exponent  $\phi$  is to look at the behavior of the dominant complex zero of the partition function [9,41–43]. The dominant zero is the one which, in the thermodynamic limit, will pinch the positive real axis at the transition temperature. The real and imaginary parts of the zero behave, including the leading order and the first correction to scaling, as

$$T_r = T_c + N^{-\phi} A_r(x) [1 + N^{-\omega} B_r(x)], \quad (22)$$

$$T_i = N^{-\phi} A_i(x) [1 + N^{-\omega} B_i(x)]. \quad (23)$$

The exponent  $\omega$  corresponds to the leading correction-to-scaling exponent. The scaling functions  $A_{r,i}(x)$  and  $B_{r,i}(x)$  are analytic functions of  $x = tN^\phi$ . In practice, we calculate the zeros in terms of the relevant Boltzmann weights, for example,  $\tau = \exp(1/T)$ , as the flatPERM method gives us a polynomial in  $\tau$ . The complex zeros of this polynomial are then calculated using the MPSOLVE package [44,45].

The scaling form (22) will apply to all the finite-size estimates of temperature for suitably chosen scaling functions  $A(x)$  and  $B(x)$  [46]. If  $\omega < \phi$ , then the leading correction will come from setting  $x = 0$  into  $A$  and  $B$ , but otherwise it might be necessary to consider a Taylor expansion of  $A$  and  $B$ . Using the definition of  $x = tN^\phi$  and rearranging gives

$$T_N = T_c + a_1 N^{-\phi} + a_2 N^{-2\phi} + b_1 N^{-\omega-\phi} + b_2 N^{-\omega-2\phi} \dots \quad (24)$$

## III. RESULTS

One of the advantages of the flatPERM stochastic enumeration method is that you calculate the coefficients of the

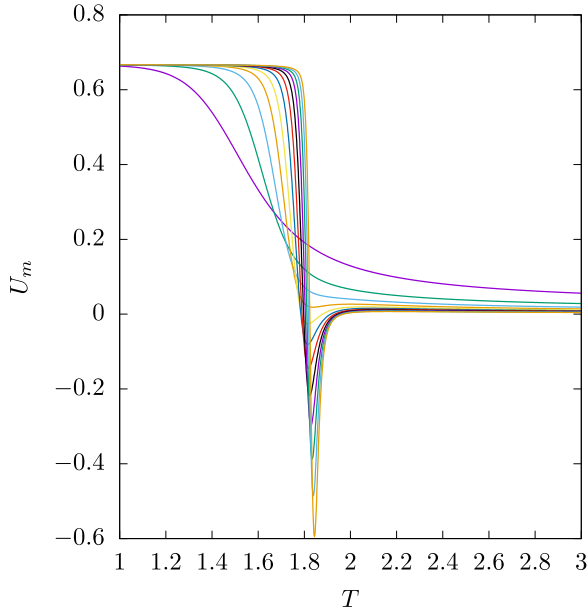


FIG. 2. Binder cumulant plotted for  $h = 0$  in three dimensions for  $N = 50$  to  $N = 600$  in steps of 50.

series expansion in terms of the dependent variables  $1/T$  and  $\tilde{h} = h/T$ . This means that you can plot quantities of interest as functions of these parameters, and not simply as isolated points as in traditional Monte Carlo methods, including those used by Garel *et al.* in Ref. [11]. There is a price to be paid, however, which is that the more dependent variables you keep track of, the slower the method is to converge, and the shorter the maximal chain length attainable in practical times. It is, therefore, useful to take cuts at fixed values of  $\tilde{h}$  to be able to explore longer chains. Here we do simulations both keeping track of  $n_i$  and  $n_s$  and, with  $h = 0$ , keeping track of only  $n_i$ . The longest chains we consider are of length  $N = 600$  in three dimensions and  $N = 1000$  in two dimensions. Typically we looked at ten independent runs of about  $10^7$  tours each. The ten different runs were used to ensure that the results had converged, and the final results used a series that was an average over the ten sets.

### A. Three-dimensional magnetic self-avoiding walks

The Binder cumulant is shown in Fig. 2. It displays a characteristic negative spike, indicative of a first-order transition [32].

We calculated the different finite-size estimates of the transition temperature using several methods: Nightingale phenomenological renormalization group [40] with the scaling relations (21), and looking at the maximum of the specific heat and the real part of the leading complex partition function zero. We also used the minimum of  $U_m$  as an indicator of the transition temperature (the bottom of the spike). These estimates are shown in Fig. 3.

For a first-order transition, we expect, to leading order, the finite-sized estimates  $T_N$  to scale with  $N^{-1}$ ; in other words, we might expect a scaling form similar to that in Eq. (24) with  $\phi = 1$ . Looking at leading-order terms, we found that the estimated values for  $T_c$  depended very weakly on  $\omega$ , and we

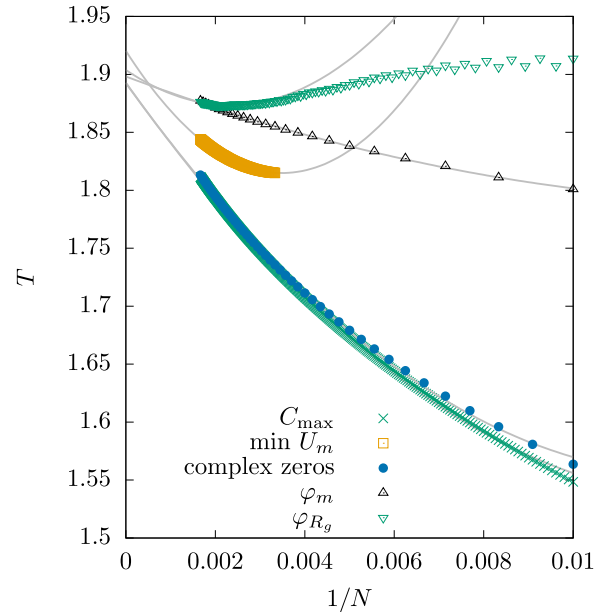


FIG. 3. Finite-size estimates of the critical temperature derived from crossings of  $\varphi_{R_g}$ ,  $\varphi_m$ , and  $C_{\max}$  and the minimum of  $U_m$ , as well as the locus of the dominant zero of the partition function as a function of  $1/N$ . The solid lines are quadratic fits to the estimates corresponding to larger values of  $N$ , which corresponds to choosing the correction-to-scaling exponent  $\omega = 1$ .

found, in particular, that setting  $\omega = -1$  gave a similar order of accuracy in the results. A similar weak dependence is found in the case of the adsorption transition in self-avoiding walks [43,47,48]. In particular, Taylor and Luettmer-Strathmann [43] chose a quadratic fit in order to take into account the correction to scaling. In Fig. 3 we show quadratic fits to the estimates corresponding to larger values of  $N$ . We varied the range of  $N$  values to obtain a good fit over the widest range of values. The estimates of  $T_c$  from such an extrapolation range from 1.89 to 1.92.

As an alternative method, we also looked at the locus of the leading complex zero in the complex plane [49–51]. In Fig. 4 we plotted the zeros in terms of the Boltzmann weight  $\tau = \exp(1/T)$ . Expanding  $\tau_r$  as a function of powers of  $N^{-\phi}$ , and using  $\tau_i \propto N^{-\phi}$ , we can look at fitting  $\tau_r$  as a polynomial in  $\tau_i$  to extrapolate to  $\tau_i \rightarrow 0$ . In Fig. 4 we used the two leading terms with  $\omega = 0.001$  and  $\omega = 1$  (i.e., a quadratic equation in  $N^{-1}$ ). The value of  $\omega = 0.001$  was chosen as it gave the best fit of most of the points in the plot. We also set  $\omega = 1$  and took as many terms in Eq. (24) as needed to fit all the points. This gave us a quartic polynomial in  $N^{-1}$ . Extrapolations using these three approximation methods gave  $\tau_c = 1.698$  ( $\omega = 0.001$ ),  $\tau_c = 1.712$  ( $\omega = 1$ ), and  $\tau_c = 1.707$  (quartic fit) or estimates of the transition temperatures of  $T_c = 1.89$ ,  $T_c = 1.86$ , and  $T_c = 1.87$ , respectively.

To confirm these exponents, we have defined the reduced temperature as

$$t = \frac{T_c - T}{T_c}$$

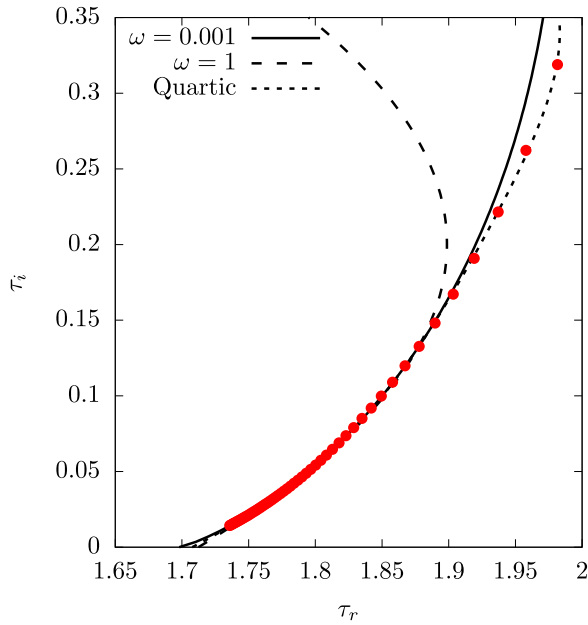


FIG. 4. Estimates of the critical temperature for  $h = 0$  by extrapolation of  $\tau_r$  as  $\tau_i \rightarrow 0$  where  $\tau = \exp(1/T)$ . Points fitted using  $\omega = 0.001$  (solid line) and  $\omega = 1$  (dashed line). The limiting values of  $\tau_r$  found where  $\tau_c = 1.698$  and  $\tau_c = 1.712$ , respectively, or  $T_c = 1.89$  and  $T_c = 1.86$ , respectively.

and plotted  $C_N/N$  against  $tN$  and  $r^2/N$  against  $tN$ . The best collapse at  $t = 0$  was achieved with  $T_c = 1.9$ . These curves are shown in Figs. 5 and 6. It is curious that the scaling of  $C$  and  $U_m$  indicate clearly a first-order transition with  $\phi = 1$ , while the scaling radius of gyration seems to indicate  $\nu = 1/2$ , as with the usual tricritical collapse.

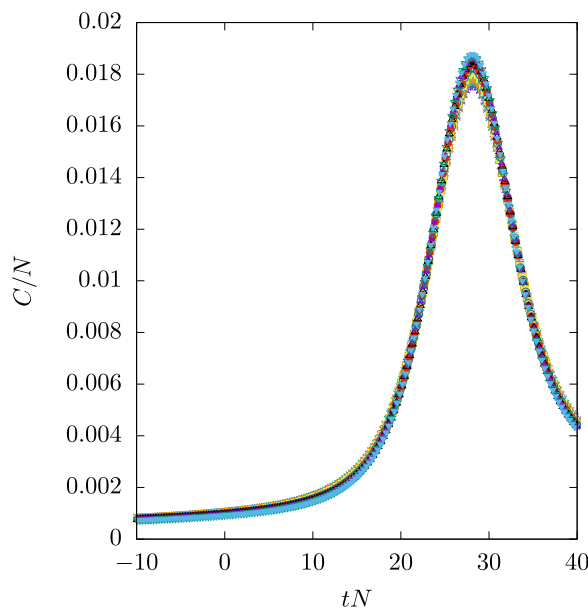


FIG. 5. Scaled specific heat  $C/N$  plotted against the scaled reduced temperature  $tN$  with  $T_c = 1.9$  and sizes from  $N = 500$  to  $N = 600$  in steps of 10.

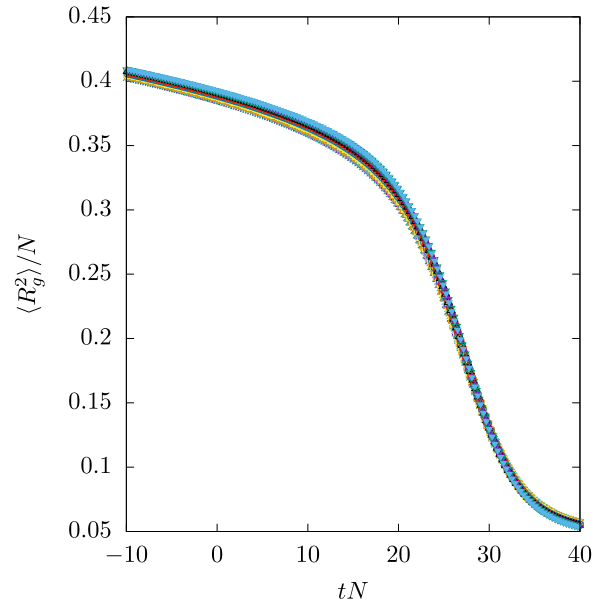


FIG. 6. Scaled radius of gyration  $\langle R_g^2 \rangle / N$  against scaled reduced temperature  $tN$  with  $T_c = 1.9$  and sizes from  $N = 500$  to  $600$  in steps of 10.

To investigate this further, we looked at the probability distributions for different temperatures (or  $\beta = 1/T$ ). In order to calculate the probability distribution for  $M$  (Fig. 7) we need the full histogram in  $n_i$  and  $n_s$ , and we were limited to 200, while we also looked at the probability distribution for the energy [expressed as  $n_i/(3N)$ ] for  $N = 600$  (Fig. 8). For the magnetization, we can clearly see the coexistence of three phases at  $\beta = 0.59$  or  $T = 1.69$ , and in the energy distribution we can see clearly the coexistence of two phases, one with a small number of contacts and one with a larger number of

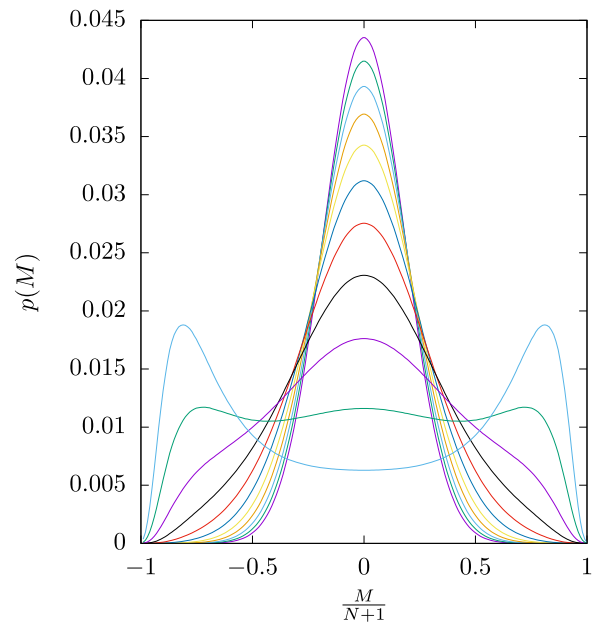


FIG. 7. Probability distributions of  $M$  for  $\beta$  from 0.5 to 0.6 in steps of 0.01 for  $N = 200$ . The plots would put the transition at about  $\beta = 0.51$  or  $T = 1.96$ .

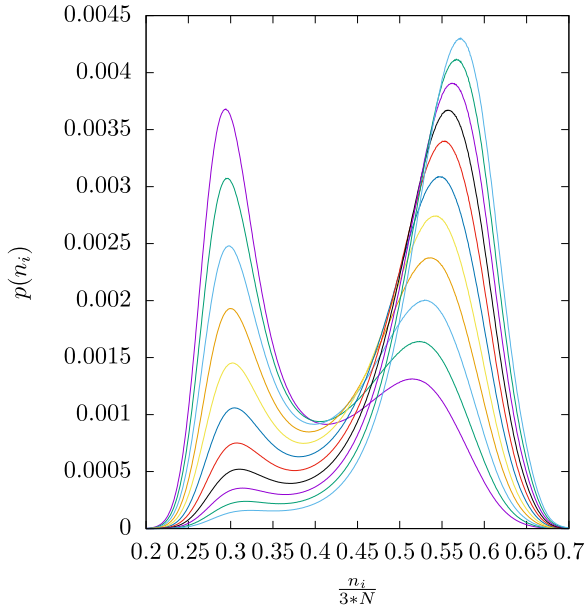


FIG. 8. Probability distributions of  $n_i$  for  $\beta$  from 0.55 to 0.56 in steps of 0.001 for  $h = 0$  for  $N = 600$ . The peaks cross over in height between  $\beta = 0.552$  and  $\beta = 0.553$ , or  $T = 1.80$  and  $1.81$ .

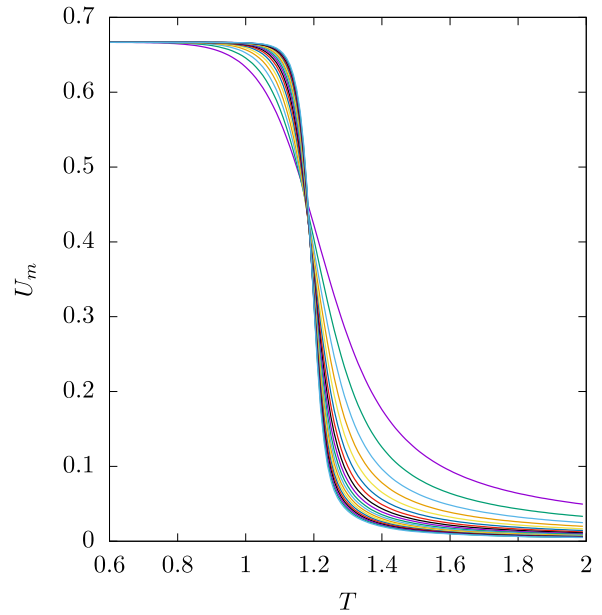


FIG. 9. Binder fourth-order cumulant as a function of  $T$  for sizes up to  $N = 1000$ .

contacts, which we interpret as swollen and collapsed phases. This latter explains the three peaks in the magnetization: when the walk is extended, the Ising model is essentially one dimensional, and cannot order, giving a zero average magnetization, while when the walk collapses, the support is three dimensional, and the Ising model is already in the magnetized phase. The tip-over point in energy occurs for  $\beta$  between 0.52 and 0.53 ( $T = 1.92$  and  $T = 1.88$ ) for  $N = 600$ . Note that the lower temperature for the magnetization is mainly because of the smaller size of walk considered. It remains interesting to note that, while the collapse transition as well as the magnetic transition occur together, the average radius of gyration, taken across the two coexisting phases, still gives an exponent  $\nu = 1/2$  for the radius of gyration.

**B. Two-dimensional magnetic self-avoiding walks**

In Fig. 9 we show the Binder cumulant for  $h = 0$  in two dimensions. This shows the form expected for a continuous phase transition, with the absence of the spike seen in the three-dimensional case. To explore this further, in Fig. 10 we explore at the probability distribution  $p(M)$ , where  $M$  is the magnetization, for different values of  $\beta = 1/T$ . The peaks show clearly the two-phase region for  $\beta > 0.835$  and the one-phase region for  $\beta < 0.835$ . When  $\beta = 0.835$ , the profile is essentially flat without the three-peak structure seen in the 3D case (Fig. 7). The probability distribution of the energy (not shown) also shows no evidence of coexistence between low-temperature and high-temperature phases. We conclude that the transition at  $h = 0$  is continuous in two dimensions, unlike what was observed in three dimensions. This leads us to conclude that the transition will be around  $T = 1/0.835 \approx 1.2$ .

Estimates of the transition temperature are calculated and shown in Fig. 11 using various methods: phenomenological

renormalization group, using the finite-size scaling forms of different quantities such as  $\varphi_m$  and  $\varphi_{R_g}$ ; and crossings of  $U_m$  and the location of the peaks of  $C$  and the magnetic susceptibility  $\chi$ , defined through

$$\chi = \frac{1}{TN} (\langle M^2 \rangle - \langle |M| \rangle^2). \tag{25}$$

We can gain an idea of the crossover exponent by looking at the scaling of the imaginary part of the complex Boltzmann weight  $\tau = \exp(-1/T)$ , calculated from the leading zero of the partition function  $Z_N$  as before. This is expected to behave

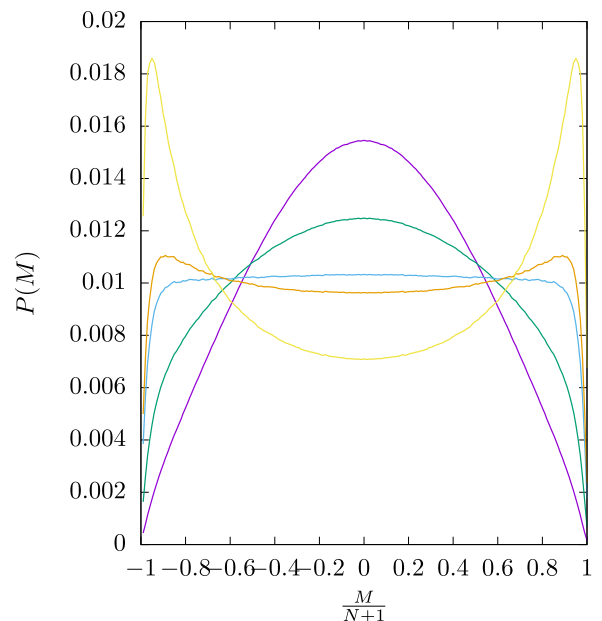


FIG. 10.  $p(M)$ , the probability distribution for five different values of  $\beta$ :  $\beta = 0.8, 0.82, 0.835, 0.84,$  and  $0.86$  for  $N = 200$ .

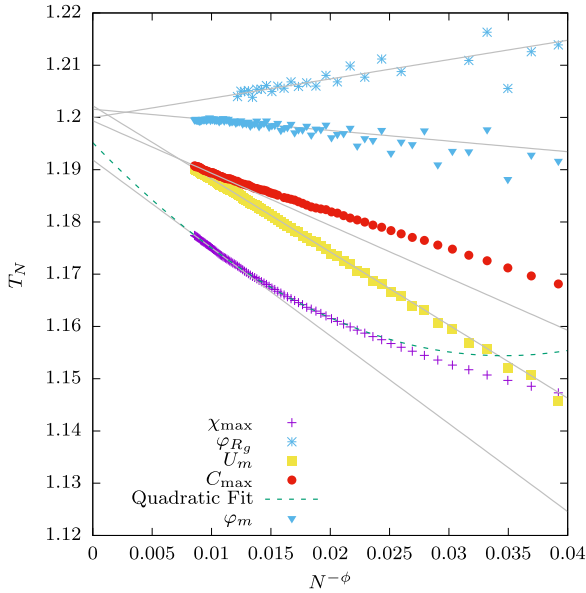


FIG. 11. Different estimates of the transition for  $h = 0$  using Binder's cumulant  $U_N$ , the scaling functions  $\varphi_m$  and  $\varphi_{R_g}$ , and the locations of the peaks of  $C$  and  $\chi$ . The lines are linear fits in  $N^{-\phi}$  to the data set ( $\varphi_m$  and  $\varphi_{R_g}$ ) or the large  $N$  values where the curves are approximately linear. The dashed line is a quadratic fit in  $N^{-\phi}$  to the larger  $N$  values for  $\chi$  in  $N^{-\phi}$  with  $\phi = 0.689$ .

as  $\tau_i \sim N^{-\phi}$ , which leads to an estimate of  $\phi \approx 0.689$ . This estimate is found by fitting the  $\ln \tau_i$  vs  $\ln N$  for large  $N$  ( $\ln N > 6$ ). Varying the slope of the fitted line around this value gives a range of acceptable values of around  $\phi = 0.7 \pm 0.03$ . The best fits in this section were found using  $\phi = 0.689$  for the finite sizes we have here. The finite-sized estimates are fitted by quadratics in  $tN^\phi$ , except the estimates from the peaks of  $\chi_N$ , which were fitted with a cubic in  $tN^\phi$ . The corresponding lines are also shown in Fig. 11. Using  $\phi = 0.689$ , the fits give extrapolated temperatures leading to  $T_c = 1.199 \pm 0.003$ .

Figure 12 shows the magnetization calculated at the estimates of  $T_c$  for both crossings of  $\varphi_m$  and  $U_m$ . The solid lines are plotted using the form  $m_N = AN^{-1/8}$ , and the fit to the curve is very good. A direct calculation of the  $\beta\phi$  estimates from the crossings of  $\varphi_m$  give results consistent with  $\beta\phi = 1/8$ . It is curious that  $\beta\phi$  should be so close to the exact value of  $\beta = 1/8$  for the two-dimensional Ising model.

We further check on the exponents by looking at the data collapse of the magnetization curves, shown in Fig. 13. We obtain good collapse of the data using  $\beta\phi = 1/8$ ,  $\phi = 0.689$ , and  $T_c = 1.201$ .

Figure 14 shows the un-normalized density calculated at the finite-size estimates of  $T_c$  plotted against  $N^{1-2\nu}$  with  $\nu = 0.585$ . The exponent  $1 - 2\nu$  is chosen by finding a best fit of the log-log curve of  $\rho_c$  against  $N$  for large enough  $N$ . The fit is seen to be good, with  $\nu = 0.585 \pm 0.01$ , slightly higher than the usual collapse transition value of  $\nu = 4/7 \approx 0.5714 \dots$ . A direct calculation of  $\nu_N$  from the crossings of  $\varphi_{R_g}$  gives a cloud of estimates, which converge as  $N$  increases. The convergence is consistent with either  $\nu = 4/7$  or  $\nu = 0.585$ .

In Fig. 15 we plot the magnetic susceptibility, which shows peaks growing and approaching the critical temperature  $T_c \approx$

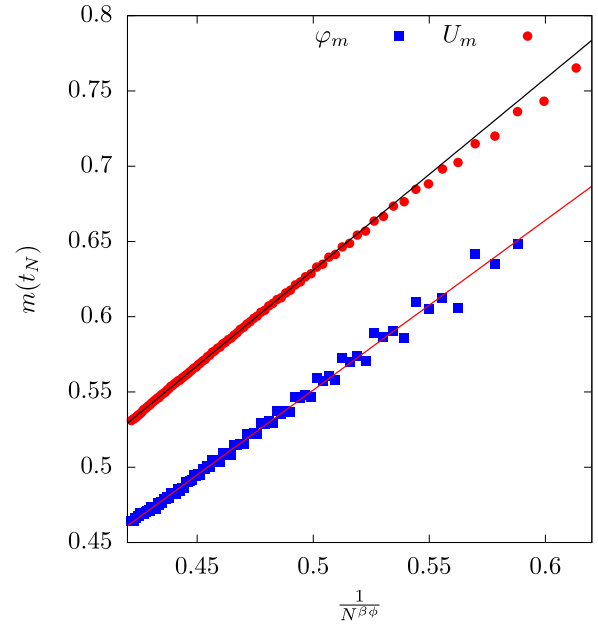


FIG. 12. Magnetization calculated at the finite-size estimate of the critical temperature from the crossings of  $\varphi_m$  and the Binder cumulant plotted as a function of  $N^{-\beta\phi}$  with  $\beta\phi = 1/8$ .

1.2. In Fig. 16 we plot the log of  $\chi_{\max}$  against  $\log N$  and fit to a straight line to get an estimate of  $\gamma\phi$ . We find  $\gamma\phi = 0.905$  from the fit, but this could drop a little. We fitted the portion of the line from  $\ln N = 6$ , and the asymptotic slope might be a little steeper. Taking the expression of  $\phi = 0.689$  would give  $\gamma = 1.31$ . Using the higher and lower limits of  $\phi = 0.69 \pm 0.02$  leads to  $\gamma = 1.31 \pm 0.03$ . In the same figure, we plot  $\ln C_{\max}$  against  $\ln N$ . Likewise, fitting with a straight line gives  $\alpha\phi = 0.365$ . Using  $\alpha = 2 - 1/\phi$ , we find  $\phi = 0.683$ , which confirms the value of  $\phi$  found from the complex partition function zeros, and  $\alpha = 0.54 \pm 0.01$ .

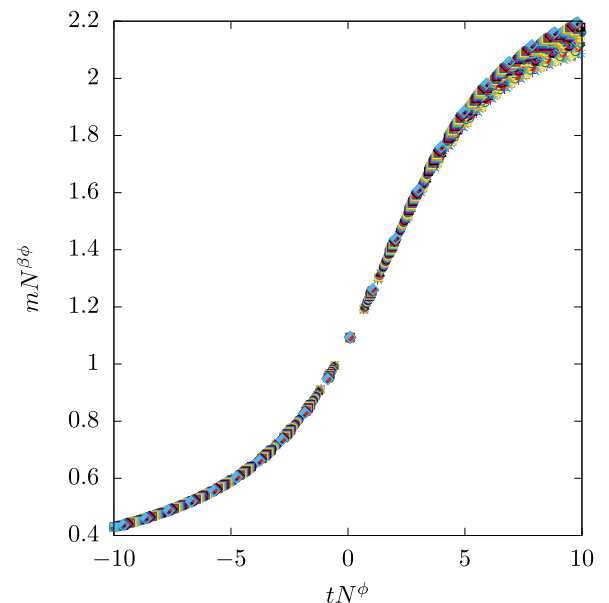


FIG. 13. Scaled magnetization  $mN^{\beta\phi}$  with  $\beta\phi = 1/8$ ,  $\phi = 0.689$ , and  $T_c = 1.201$  with  $N$  from 500 to 1000 in steps of 10.

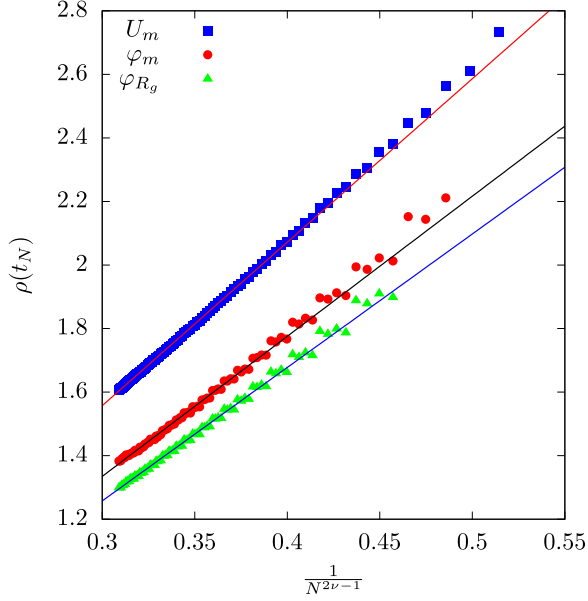


FIG. 14. The value of the un-normalized density  $\rho_c = N/(R_g^2)$  measured at the crossing value of  $\varphi_{R_g}$  and  $\varphi_m$  for  $N, N/2$  and  $N/2, N/4$  as well as at the crossings of  $U_m$  for  $N$  and  $N/2$ . The estimates are plotted as a function of  $N^{1-2\nu} = N^{-0.17}$  or  $\nu = 0.585$ .

Since we have the full set of effective coefficients  $C_{N,n}^{\text{eff}}$  up to  $N = 1000$ , we can look at the cutoff grand-canonical partition functions

$$\mathcal{Z}_N = \sum_{l=0}^N K^l Z_l. \quad (26)$$

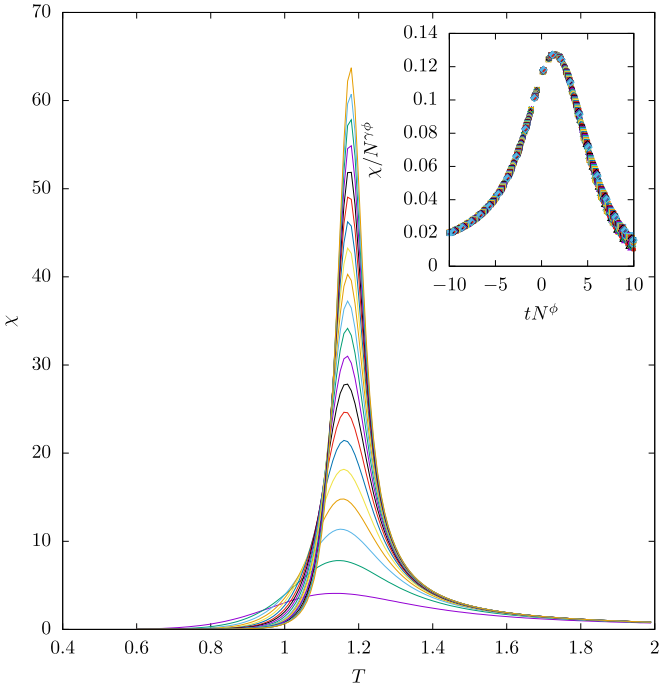


FIG. 15. Magnetic susceptibility  $\chi$  plotted against  $T$  for sizes from 50 to  $N = 1000$  in steps of 50. The inset shows the scaled susceptibility  $\chi/N^{\gamma\phi}$  vs  $tN^\phi$  with  $T_c = 1.192$ ,  $\gamma\phi = 0.9$ , and  $\phi = 0.689$  with  $N$  from 500 to 1000 in steps of 10.

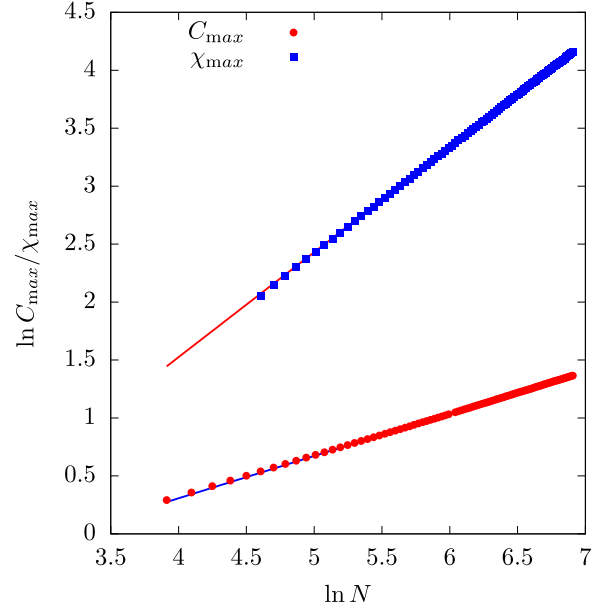


FIG. 16.  $\ln(\chi_{\max})$  and  $\ln C_{\max}$  plotted vs  $\ln(N)$ . The slope of the line is fitted to a line of slope  $\gamma\phi = 0.905$  for  $\chi_{\max}$  and  $\alpha\phi = 0.365$  for  $C_{\max}$ .

$N$  here is the maximum length taken into account in the cutoff partition function. The canonical partition function is expected to scale like

$$\mathcal{Z}_N \sim \mu^N N^{\gamma_{\text{pol}}-1}, \quad (27)$$

where  $\gamma_{\text{pol}}$  is the polymer entropic exponent, not the exponent related to the magnetic susceptibility, defined above. The naming convention comes from the identification of the walk configurations in  $\mathcal{Z}$ , the grand-canonical partition function, as the graphs coming from the high-temperature expansion of the susceptibility of the  $O(n = 0)$  spin model [5].

Substituting into Eq. (26) gives the grand-canonical scaling behavior

$$\mathcal{Z} \sim (K_c - K)^{-\gamma_{\text{pol}}}. \quad (28)$$

Using the scaling of average length with  $K$ , which is now limited by the cutoff in length, gives the finite-size scaling relation

$$\mathcal{Z} \sim N^{-\gamma_{\text{pol}}}. \quad (29)$$

We can define a phenomenological scaling function:

$$\varphi_{\gamma_{\text{pol}}} = \frac{\ln\left(\frac{\mathcal{Z}_N}{\mathcal{Z}_{N/2}}\right)}{\ln 2}. \quad (30)$$

The crossings of these functions will give estimates of both  $\gamma_{\text{pol}}$  and  $K_c$ . Figure 17 shows, for each value of  $T$  shown in the critical region, the estimated  $\gamma(T)$  calculated from the crossings of  $\varphi_{\gamma_{\text{pol}}}$  for  $N/(N/2)$  with  $(N/2)/(N/4)$  plotted for different values of  $N$  in the critical region. Intersections of these estimates will further pick out estimates for  $T_c^N$ . Looking at the intersections and extrapolating leads to an estimate of  $T_c \approx 1.202$ . This can be examined further by fixing the expected critical temperature and looking at the estimate of  $\gamma_{\text{pol}}$  as a function of length. If we are at the critical temperature,



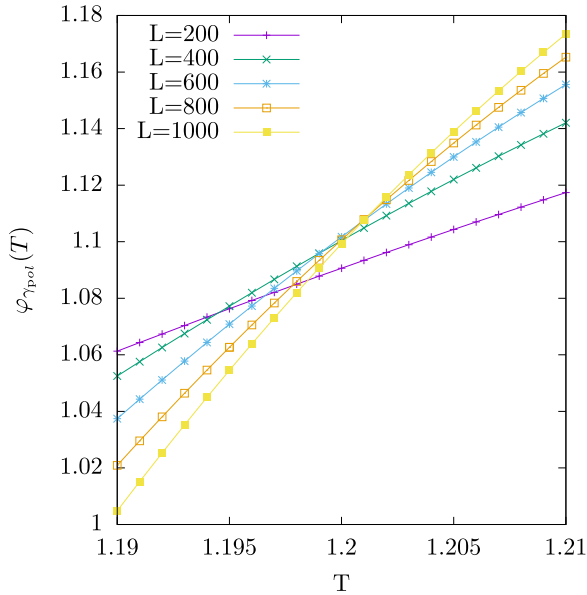


FIG. 17.  $\varphi_{\gamma_{\text{pol}}}$  for sizes  $N = 200, 400, 600, 800,$  and  $1000$ .

the exponent value is expected to be linear in  $N$  for large  $N$ , from the linearity of  $k = (K_c - K)/K_c$  in  $N$ . If we are off the critical temperature, but close, the smaller sizes will be in the critical region, but as the length increases, this region becomes smaller, and the walk is subject to crossover effects, pulling the estimate off linearity. This is shown in Fig. 18, where the best fit to a linear line up to  $N = 1000$  is  $T_c = 1.2025$ , which is a little higher than found with the canonical analysis above, but still within the expected error bars. This gives  $\gamma_{\text{pol}} = 1.1255 \pm 0.003$ , which is a little smaller than the exact value of  $\gamma_{\text{pol}} = 8/7 \approx 1.143$  at the standard collapse transition, but fairly close to it.

IV. DISCUSSION

In this paper we have revisited the three-dimensional magnetic polymer, realized by a chain of Ising spins along the backbone of a fluctuating walk, with the Ising energy as the sole interaction energy. We have produced improved numerical results, which clearly show the nature of the first-order simultaneous collapse and magnetic transition. Both appear to be first order, but the average radius of gyration still scales as  $R_g \sim N^{1/2}$ , rather than  $R_g \sim N^{1/3}$  as expected for a dense walk. The mean-field theory of Garel *et al.* [11] predicts a first-order transition for small  $h$ , becoming the standard collapse transition for larger  $h$ . They claim that the first-order transition exists for finite, nonzero, magnetic field, based on the scaling of the specific heat. We find similar results, but when we look at the probability distribution of both  $m$  and  $n_i$ , even with  $h/T = 0.1$ , there is only a marginal sign of the possible

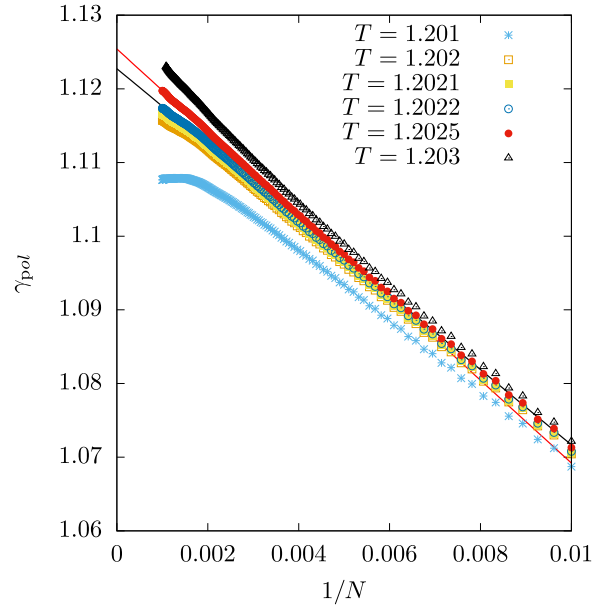


FIG. 18. Plots of estimates of  $\gamma_{\text{pol}}$  as a function of  $1/N$  for different temperatures around the critical temperature estimated from  $\varphi_{\gamma_{\text{pol}}}$ .

existence of a finite-size first-order transition. The question of a finite  $h$  first-order transition is, in our mind, still open.

This MFT does not restrict the model to a single walk and equally applies to a “gas” of walks, and it might be interesting to see how removing the restriction of a single walk affects the behavior in both two and three dimensions.

When the three-dimensional model is changed to introduce more fluctuations, such as the fluctuating bond model studied by Luo [28], the first-order transition gives way to a second-order transition. If we reexamine their scaling relations and realize that they should have used  $\phi$  and not  $1/\nu$  in their scaling relations, we reinterpret their results as being  $\phi = 1$  and  $\beta \approx 1/3$ , to be compared with the three-dimensional Ising value of  $\beta \approx 0.326$ . In two dimensions, fluctuations are also more important, and again, we see a second-order transition. Interestingly, while we find a value of  $\phi \approx 0.69 \neq 1$ , the magnetic transition is characterized by the exponent  $\beta\phi = 1/8$ , to be compared with  $\beta = 1/8$  for the usual transition. This warrants further investigation.

In two dimensions, we could find no evidence that there is a magnetic transition for  $h \neq 0$ , and it would seem likely that for  $h \neq 0$  the transition is the usual collapse transition. The geometric and entropic exponents found for the walk with  $h = 0$ ,  $\nu$  and  $\gamma_{\text{pol}}$ , are close to, but not the same as, the usual  $\theta$ -point exponent values. This discrepancy could be due to finite-size effects.

The following table summarizes the results presented:

	$T_c$	$\alpha$	$\phi$	$\gamma$	$\nu$	$\gamma_{\text{pol}}$
2D	$1.199 \pm 0.003$	$0.54 \pm 0.01$	$0.69 \pm 0.02$	$1.31 \pm 0.03$	$0.585 \pm 0.01$	$1.1255 \pm 0.0003$
3D	$1.90 \pm 0.02$	1	1	–	1/2	–

In the model presented here, the magnetic and collapse transitions occur together. It is simple to imagine a model where these two transitions, with different order parameters, might occur separately, which might give interesting additional critical behaviors.

Recently a dynamic HP model has been studied in two dimensions [52]. This model is similar in that both the hydrophobic (H) and the polar (P) state of each monomer and the conformation are dynamic variables. The main difference with the work here is that there is not an interaction along the chain, only between nonconsecutive nearest-neighbor monomers of

type P. They found that the collapse transition here was in the standard  $\theta$  universality class.

*Note added.* A parallel piece of work on this model in two dimensions has recently been reported by Faizullina, Pchelintsev, and Burovski [53]. The results they found support the results we present within quoted error bars.

#### ACKNOWLEDGMENT

The authors thank Martin Weigel for useful comments.

- 
- [1] C. Vanderzande, *Lattice Models of Polymers*, Cambridge Lecture Notes in Physics (Cambridge University, Cambridge, England, 1998).
- [2] P. G. d. de Gennes, Collapse of a polymer chain in poor solvents, *J. Phys., Lett.* **36**, 55 (1975).
- [3] M. Stephen, Collapse of a polymer chain, *Phys. Lett. A* **53**, 363 (1975).
- [4] B. Duplantier, Lagrangian tricritical theory of polymer chain solutions near the  $\theta$  point, *J. Phys. Fr.* **43**, 991 (1982).
- [5] H. W. J. Blote and B. Nienhuis, Critical behaviour and conformal anomaly of the O(n) model on the square lattice, *J. Phys. A: Math. Gen.* **22**, 1415 (1989).
- [6] D. P. Foster and C. Pinettes, A corner transfer matrix renormalization group investigation of the vertex-interacting self-avoiding walk model, *J. Phys. A: Math. Gen.* **36**, 10279 (2003).
- [7] D. P. Foster and C. Pinettes, Surface critical behaviour of the vertex-interacting self-avoiding walk on the square lattice, *J. Phys. A: Math. Theor.* **45**, 505003 (2012).
- [8] A. Bedini, A. L. Owczarek, and T. Prellberg, Numerical simulation of a lattice polymer model at its integrable point, *J. Phys. A: Math. Theor.* **46**, 265003 (2013).
- [9] D. Foster, R. Kenna, and C. Pinettes, Use of the complex zeros of the partition function to investigate the critical behavior of the generalized interacting self-avoiding trail model, *Entropy* **21**, 153 (2019).
- [10] É. Vernier, J. L. Jacobsen, and H. Saleur, A new look at the collapse of two-dimensional polymers, *J. Stat. Mech.* (2015) P09001.
- [11] T. Garel, H. Orland, and E. Orlandini, Phase diagram of magnetic polymers, *Eur. Phys. J. B* **12**, 261 (1999).
- [12] D. Michieletto, E. Orlandini, and D. Marenduzzo, Polymer Model with Epigenetic Recoloring Reveals a Pathway for the *de Novo* establishment and 3D Organization of Chromatin Domains, *Phys. Rev. X* **6**, 041047 (2016).
- [13] D. Michieletto, E. Orlandini, and D. Marenduzzo, Epigenetic transitions and knotted solitons in stretched chromatin, *Sci. Rep.* **7**, 14642 (2017).
- [14] D. Michieletto, D. Coli, D. Marenduzzo, and E. Orlandini, Nonequilibrium Theory of Epigenomic Microphase Separation in the Cell Nucleus, *Phys. Rev. Lett.* **123**, 228101 (2019).
- [15] D. Mostarac, P. A. Sánchez, and S. Kantorovich, Characterisation of the magnetic response of nanoscale magnetic lamellae in applied fields, *Nanoscale* **12**, 13933 (2020).
- [16] É. Bereczk-Tompa, F. Vonderviszt, B. Horváth, I. Szalai, and M. Pósfai, Biotemplated synthesis of magnetic filaments, *Nanoscale* **9**, 15062 (2017).
- [17] A. Grein-Iankovski, A. Graillot, M. Radiom, W. Loh, and J.-F. Berret, Template-free preparation of thermoresponsive magnetic cilia compatible with biological conditions, *J. Phys. Chem. C* **124**, 26068 (2020).
- [18] G. Z. Archontis and E. I. Shakhnovich, Phase transitions in heteropolymers with “secondary structure”, *Phys. Rev. E* **49**, 3109 (1994).
- [19] B. K. Chakrabarti and S. Bhattacharya, Study of an ising model on a self-avoiding-walk lattice, *J. Phys. C* **16**, L1025 (1983).
- [20] S. Bhattacharya and B. K. Chakrabarti, Ising model on self-avoiding walk chains, *Z. Phys. B* **57**, 151 (1984).
- [21] B. K. Chakrabarti, A. C. Maggs, and R. B. Stinchcombe, Ising model on a self-avoiding walk, *J. Phys. A: Math. Gen.* **18**, L373 (1985).
- [22] M. C. Tesi, E. J. J. van Rensburg, E. Orlandini, and S. G. Whittington, Interacting self-avoiding walks and polygons in three dimensions, *J. Phys. A: Math. Gen.* **29**, 2451 (1996).
- [23] E. Orlandini, Monte Carlo study of polymer systems by multiple Markov chain method, in *Numerical Methods for Polymeric Systems* (Springer, New York, 1998), pp. 33–57.
- [24] M.-B. Luo, Monte Carlo study on the statistical properties of Ising polymer chain, *Int. J. Mod. Phys. B* **17**, 4267 (2003).
- [25] M.-B. Luo and J.-H. Huang, Monte Carlo simulation of polymer chain with ferromagnetic ising interaction, *J. Chem. Phys.* **119**, 2439 (2003).
- [26] J.-H. Huang and M.-B. Luo, Monte Carlo simulation of the response of ferromagnetic polymer chain to external magnetic field, *Polymer* **45**, 2863 (2004).
- [27] J.-H. Huang, M.-B. Luo, and C.-J. Qian, Curie temperature of a ferromagnetic polymer chain model, *J. Appl. Polym. Sci.* **99**, 969 (2005).
- [28] M.-B. Luo, Finite-size scaling analysis on the phase transition of a ferromagnetic polymer chain model, *J. Chem. Phys.* **124**, 034903 (2006).
- [29] M.-B. Luo and C.-J. Qian, Short-time monte carlo study on the phase transition of a ferromagnetic polymer chain model, *Polymer* **47**, 1451 (2006).
- [30] P. Grassberger, Pruned-enriched Rosenbluth method: Simulations of  $\theta$  polymers of chain length up to 1 000 000, *Phys. Rev. E* **56**, 3682 (1997).

- [31] T. Prellberg and J. Krawczyk, Flat Histogram Version of the Pruned and Enriched Rosenbluth Method, *Phys. Rev. Lett.* **92**, 120602 (2004).
- [32] K. Binder and D. W. Heermann, *Monte Carlo Simulation in Statistical Physics: An Introduction* (Springer, Cham, Switzerland, 2010).
- [33] K. Binder, Finite size scaling analysis of ising model block distribution functions, *Z. Phys. B* **43**, 119 (1981).
- [34] K. Binder, Critical Properties from Monte Carlo Coarse Graining and Renormalization, *Phys. Rev. Lett.* **47**, 693 (1981).
- [35] X. S. Chen and V. Dohm, Nonuniversal finite-size scaling in anisotropic systems, *Phys. Rev. E* **70**, 056136 (2004).
- [36] W. Selke, Critical binder cumulant of two-dimensional Ising models, *Eur. Phys. J. B* **51**, 223 (2006).
- [37] J. Cardy, *Scaling and Renormalization in Statistical Physics*, Cambridge Lecture Notes in Physics (Cambridge University, Cambridge, England, 1996).
- [38] P. M. Lam, Specific heat and collapse transition of branched polymers, *Phys. Rev. B* **36**, 6988 (1987).
- [39] B. Duplantier, Geometry of polymer chains near the theta-point and dimensional regularization, *J. Chem. Phys.* **86**, 4233 (1987).
- [40] M. Nightingale, Scaling theory and finite systems, *Phys. A (Amsterdam, Neth.)* **83**, 561 (1976).
- [41] J. H. Lee, S.-Y. Kim, and J. Lee, Exact partition function zeros and the collapse transition of a two-dimensional lattice polymer, *J. Chem. Phys.* **133**, 114106 (2010).
- [42] M. Ponmurugan and S. V. M. Satyanarayana, The  $\theta$  points of interacting self-avoiding walks and rings on a 2D square lattice, *J. Stat. Mech.* (2012) P06010.
- [43] M. P. Taylor and J. Luettmmer-Strathmann, Partition function zeros and finite size scaling for polymer adsorption, *J. Chem. Phys.* **141**, 204906 (2014).
- [44] D. A. Bini and L. Robol, Solving secular and polynomial equations: A multiprecision algorithm, *J. Comput. Appl. Math.* **272**, 276 (2014).
- [45] D. Bini and G. Fiorentino, Design, analysis, and implementation of a multiprecision polynomial rootfinder, *Numer. Algorithms* **23**, 127 (2000).
- [46] F. J. Wegner, Corrections to scaling laws, *Phys. Rev. B* **5**, 4529 (1972).
- [47] J. A. Plascak, P. H. L. Martins, and M. Bachmann, Solvent-dependent critical properties of polymer adsorption, *Phys. Rev. E* **95**, 050501(R) (2017).
- [48] C. J. Bradly, A. L. Owczarek, and T. Prellberg, Universality of crossover scaling for the adsorption transition of lattice polymers, *Phys. Rev. E* **97**, 022503 (2018).
- [49] T. D. Lee and C. N. Yang, Statistical theory of equations of state and phase transitions. II. Lattice gas and Ising model, *Phys. Rev.* **87**, 410 (1952).
- [50] C. N. Yang and T. D. Lee, Statistical theory of equations of state and phase transitions. I. Theory of condensation, *Phys. Rev.* **87**, 404 (1952).
- [51] M. E. Fisher, *Lectures in Theoretical Physics* (University of Colorado, Boulder, CO, 1965), Chap. 1.
- [52] K. Faizullina and E. Burovski, Globule-coil transition in the dynamic HP model, *J. Phys.: Conf. Ser.* **1740**, 012014 (2021).
- [53] K. Faizullina, I. Pchelintsev, and E. Burovski, Critical and geometric properties of magnetic polymers across the globule-coil transition, arXiv:2107.11830 (2021).